# DRX over LAA-LTE-A New Design and Analysis Based on Semi-Markov Model

Mukesh Kumar Maheshwari, Abhishek Roy, *Member, IEEE*, and Navrati Saxena, *Member, IEEE*

**Abstract**—Ever-increasing demand of data rate and subscriber penetration are resulting in continuous growth of mobile data traffic. In order to meet this exponential data traffic growth 3GPP Release 13, we have decided to enable the operation of Long Term Evolution (LTE) in the unlicensed band, termed as Licensed-Assisted Access (LAA). As the unlicensed spectrum is mainly used by WiFi, LTE evolved NodeB (eNB) has to perform Listen Before Talk (LBT) procedure to access the unlicensed channel. If the unlicensed spectrum is occupied by other services, User Equipment (UE) should remain active and wait for unlicensed channel to become idle. UE consumes a high power by remaining active, when unlicensed channel is not available. The UE's energy consumption could be saved by configuring Discontinuous Reception (DRX) in the unlicensed band, similar to DRX in LTE. In this article, we introduce and analyze a new Licensed-Assisted Access DRX mechanism (LAA-DRX) over LTE networks. Using our novel four state semi-Markov model, we show the probabilistic estimation of power saving and wake up latency associated with our proposed LAA-DRX process. Mathematical analysis and simulation results, using real wireless trace, point out that comparing to existing LTE DRX process, our LAA-DRX can achieve almost 4 percent higher power savings and up to 58 percent reduction in resource usage.

**Index Terms**—Licensed-assisted access (LAA), discontinuous reception (DRX), power saving, latency, LTE, listen before talk, semi-Markov

## 1 Introduction

The number of the mobile broadband subscribers are increasing exponentially. By 2,022 there would be 8.9 billion mobile subscribers, of which 90 percent are expected to be using mobile broadband [1]. This increase requires not only high capacity in the system, but also high data rate to meet the customer's expectation. In Long Term Evolution (LTE) wireless systems, spectrum efficiency is improved by using Multiple-Input Multiple-Output (MIMO) transmission, frequency reuse, by deploying small cells and higher multiple access techniques [2]. Unfortunately, dense small cell deployment is gradually creating congestion in the licensed LTE spectrum. Thus, cellular network operators are now in need of more spectrum to meet the increasing demands. As the limited licensed spectrum is an expensive resource for the operator, a cost-effective approach to meet the rapid mobile data growth is to deploy LTE in the unlicensed band [3]. The vast availability of unlicensed spectrum promises to fill the gap of licensed spectrum bandwidth limitation. Dual connectivity between the licensed band and unlicensed band is identified as one of the key technologies for future cellular systems.

LTE networks in the unlicensed band (5 GHz) have already attracted the attention of 3GPP. This new feature is termed as Licensed-Assisted Access (LAA) to unlicensed spectrum [3]. Fig. 1 delineates that for LAA operation two carriers are used: (i) licensed carrier and (ii) unlicensed carrier (5 GHz). The unlicensed carrier is used with the assistance of licensed carrier. Currently, 5 GHz unlicensed spectrum is primarily used by WiFi, which allows higher data rate and better spectrum efficiency as compared to 2.4 GHz unlicensed spectrum [4]. Interestingly, the amount of allocated unlicensed spectrum and plan to allocate unlicensed spectrum in the near future are comparable to licensed spectrum [5]. Hence, LTE in the unlicensed spectrum might affect the performance of already existing services in the unlicensed band, such as WiFi networks. Therefore, 3GPP has clarified the coexistence requirement, such that LAA coexistence does not affect the throughput and latency of existing WiFi services. Moreover, 3GPP standards have also specified the Maximum Channel Occupancy Time (MCOT) for fair spectrum sharing [3], [4], [6], [7], [8].

*Motivation.* LAA opportunistically boosts the user throughput by carrier aggregation of both licensed and unlicensed carrier. For LAA coexistence with WiFi and other un-licensed carriers, Evolved NodeB (eNB) of LTE networks has to perform clear channel assessment before accessing the unlicensed channel and intimate the UE about the unlicensed channel. Even if eNB gets access to an unlicensed channel, the duration of transmission is limited to MCOT [3]. Since the unlicensed spectrum is used by WiFi and other operators, there is no guarantee of unlicensed channel availability for UE at the exact moment. Hence, the UE should remain active and wait for the unlicensed channel, which increases the UE energy consumption.

LTE adopts the Discontinuous Reception (DRX) for power saving in User Equipment (UE). As shown in Fig. 2, LTE DRX consists of active, short and long sleep states.

- *M.K. Maheshwari and N. Saxena are with the Electrical and Computer Engineering Department, Sungkyunkwan University, Suwon 110-745, Korea. E-mail: {mkm005, navrati}@skku.edu.*
- *A. Roy is with the System Design Lab, Networks Division, Samsung Electronics, Suwon 16677, South Korea. E-mail: abhishek.roy@samsung.com.*

*Manuscript received 2 Aug. 2017; revised 20 Apr. 2018; accepted 30 Apr. 2018. Date of publication 11 May 2018; date of current version 7 Jan. 2019. (Corresponding author: Navrati Saxena.)*
*For information on obtaining reprints of this article, please send e-mail to: reprints@ieee.org, and reference the Digital Object Identifier below.*
*Digital Object Identifier no. 10.1109/TMC.2018.2835443*

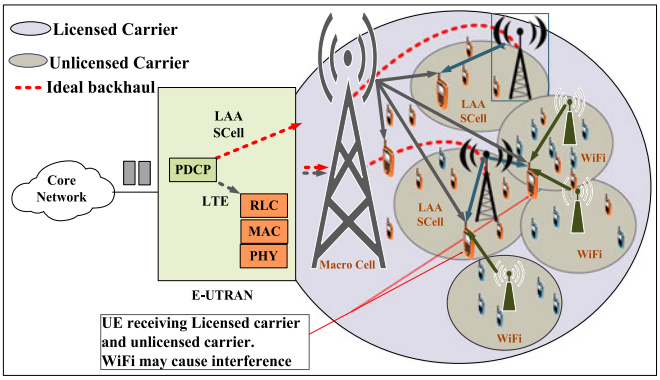


Fig. 1. Licensed Assisted Access (LAA).

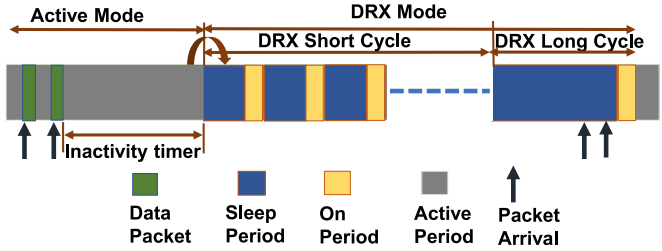


Fig. 2. LTE DRX.

DRX reduces energy consumption by allowing UE to monitor the Physical Downlink Control Channel (PDCCH) less frequently. Thus, it saves UE's power at the cost of an increase in delay [9], [10], [11], [12], [13], [14]. DRX would be even more vital in LAA enabled UEs, in view of higher energy expenses. It allows UE to transit to the sleep state, if the unlicensed band is not available or there is no packet transmission/reception during the active state. In LTE, UE navigates from sleep to active mode directly to serve the data. However, in LAA UE cannot receive the data, if an unlicensed channel is not available. UE has to wait for unlicensed channel intimation from eNB to serve the data. LTE DRX, in its current state, cannot work with LAA because it does not consider any channel access mechanism. This motivates us to redesign DRX mechanism for LTE operation in the unlicensed band. In particular, we take a step forward to answer the following fundamental questions: (a) How can we model channel idle time for LAA? (b) How can we drive analytical model of DRX for LAA? (c) How much power and resource savings could be achieved from these solutions? (d) Is the power saving versus wake up latency tradeoff in the solutions enough for real implementation? In this paper, we will discuss our answers to these fundamentals questions.

*Our Contributions.* In this paper, we first explore the Licensed Assisted Access, use cases of LTE in the unlicensed band and LTE DRX. We infer that LTE operation in the unlicensed band can boost the UE throughput, at the expense of additional energy consumption. In order to resolve the challenges associated with increased energy consumption, we introduce Discontinuous Reception over Licensed-Assisted Access (LAA-DRX). Our primary contributions are summarized below:

(1) We analyze LAA-DRX using a four-state semi-Markov model, as the associated state transition and holding time are arbitrarily distributed. Moreover, semi-Markov process model does not possess the memoryless property. The analysis provides an insight into the design of new DRX mechanism.
(2) We consider only short sleep cycle for DRX analysis, as channel access time is quite limited and unlicensed channels are occupied by other services. The short sleep cycles allow UE to get the unlicensed channel availability information more frequently.
(3) In addition to the short sleep state, we introduce a new ON state into the DRX mechanism. UE gets information about the unlicensed channel availability and packets buffered at eNB during the ON period. The probability of spectrum availability is obtained using generalized Pareto distribution [15], [16].
(4) Probabilistic estimation of performance metrics, power saving factor and wake up latency are carried out to analyze the efficiency of LAA-DRX. Subsequently, we derive the expression for resource usage during LAA-DRX.
(5) The LAA-DRX scheme is analyzed by adopting European Telecommunications Standard Institute (ETSI) traffic model [17]. Performance analysis shows that LAA-DRX reduces 58 percent resource usage, compared to LAA without DRX. Moreover, LAA-DRX achieves 4 percent gain in power saving as compared to LTE DRX.
(6) Additionally, system level simulations are also carried out to validate the analytical results. Our simulation model incorporates real trace obtained from Umass Trace Repository [18].

The rest of the paper is organized as follows. In Section 2 we present the overview of LAA, LTE DRX and associated traffic model and channel access mechanism. Section 3 introduces the new LAA-DRX proposal, semi-Markov process based analysis of power saving factor and wake up latency. The analysis of resource usage in LAA-DRX is also presented in Section 3. Section 4 demonstrates the performance evaluations based on the numerical analysis and simulation studies, conducted using real traffic trace. Finally, we conclude the paper in Section 5.

## 2 Background

In this section, we present the fundamentals of LAA and the basic operation of LTE DRX mechanism. Then we review the traffic model and channel access mechanism. The summary of related work publications in LAA, LTE DRX and channel access mechanism is provided in Table 1.

### 2.1 Overview of Licensed Assisted Access (LAA)

We first discuss the design targets, deployment scenarios and LAA radio access.

*Design Targets.* The practical way to operate LTE in the unlicensed 5 GHz band is LTE-Unlicensed (LTE-U) and Licensed-Assisted Access. LTE-U and LAA operation requires licensed carrier (primary carrier) and unlicensed carrier (secondary carrier). The licensed carrier is available all the time, while the availability of unlicensed carrier depends on the load on the unlicensed channel [3]. The early deployment of LTE-U is relatively simple and

TABLE 1
Related Works in Licensed Assisted Access and Channel Access Mechanism

| Technology in Focus | Ref. | Work Summary | Objective(s) |
|---|---|---|---|
| LAA | [2], [23] | • Overview of LAA technology of 3GPP Release 13<br>• Evaluation results of coexistence by 3GPP<br>• Solution for LAA-WiFi hidden terminal problem<br>• Game-theoretic base pricing strategy proposal | • LAA standardization activities 3GPP<br>• Key technical features of LAA |
| LAA | [7], [19], [20] | • Probabilistic analysis for LTE and WiFi operation<br>• LTE in unlicensed band boosts the capacity at the expense of degraded WiFi performance | • Coexistence challenges of LTE and WiFi<br>• Performance of LTE in unlicensed band and its impact on WiFi |
| LAA | [8], [22] | • Coexistence of WiFi and LTE with different LBT<br>• LBT adoption design for LTE in unlicensed spectrum | • LBT in unlicensed spectrum |
| DRX | [10], [11], [12], [14] | • DRX modeling based on semi-Markov chain model<br>• Analysis of DRX based on short and long cycle | • Energy saving for M2M devices<br>• Extending battery life of smart phones |
| Traffic Model | [17] | • Data traffic modeling (Pareto & Weibull distributions) | • ETSI Traffic Model proposal |
| CR | [15], [26] | • Time-dimension modeling of spectrum usage in CR<br>• Comprehensive survey of spectrum occupancy modeling<br>• Statistical properties from measured data | • Modelling of spectrum occupancy for radio communication systems |
| WLAN | [16], [27] | • Performance of spectrum utilization at ISM band<br>• Statistical characterization of the idle periods' distribution<br>• semi-Markov model proposal for idle and busy periods | • Spectrum sharing opportunities in WLAN |

does not require any changes in LTE air interface. It uses carrier aggregation protocols mentioned in 3GPP Rel 10 - 3GPP Rel 12, without any Listen Before Talk (LBT) mechanism, to access the channel. LTE-U may swamp the unlicensed band, thereby causing WiFi users, using these frequencies, to suffer. On the other hand, 3GPP Release 13 standards mention that LAA targets a single global framework to meet the regulations, e.g., LBT, channel occupancy time, power spectral density and bandwidth [3], [19], [20].

The WiFi network operates in unlicensed spectrum and deploys contention-based Carrier Sense Multiple Access Collision Avoidance (CSMA/CA) [21]. Similar to CSMA/CA, for fair coexistence, the LAA networks adopt LBT procedure. In LBT or Clear Channel Assessment (CCA), radio transmitter determines whether the medium is idle by sensing the medium. If the medium is idle, the transmission is initiated; otherwise, the UE waits for the channel to become idle. LBT detects threshold energy to determine the transmission of the signal by other types of equipment over the channel [2], [8]. LBT procedure is required in Japan and Europe, but not in the U.S and China [2], [3], [22]. For fair unlicensed spectrum access between WiFi and LAA, according to 3GPP Release 13, the CCA time is 20 $\mu$s and MCOT is 10 ms [3], [23]. The value of MCOT is different for different regions. For LAA operation in Japan and Europe, eNB needs to sense the unlicensed channel after every 4 ms, if the downlink transmission burst is longer than 4 ms [2], [3]. Hence, it is quite clear LAA functionality requires discontinuous transmission with a pre-defined MCOT.

The unlicensed 5 GHz band comprises of several chunks of bandwidth. A transmitter can a select single or multiple band for communication with a limited transmit power to avoid interference [23]. The restricted transmit power imposes restrictions and limitations on the coverage of LAA. Hence, unlicensed carrier is more suitable for small cells having smaller coverage. LAA system might also face interference with weather radar systems, operating in the same unlicensed band. In order to avoid interference, LAA uses dynamic frequency selection function by changing the carrier [3].

*Deployment Scenarios*. The unlicensed carrier is shared by WiFi and many LAA operators. Although suitable for small cells, LAA cannot match the Quality of Service (QoS) requirement compared to the licensed carrier. Therefore, in downlink, the unlicensed carrier is mostly used as a secondary carrier (supplement), assisted by a licensed carrier, by using carrier aggregation. The different operation scenarios of LAA deployment by 3GPP TR 36.889 [3] are summarized as follows:

- Fig. 3a delineates the macro cell is associated with licensed carrier and the small cell is associated with the unlicensed carrier. The RRC signal and data are exchanged by using the licensed carrier. If an UE is under small cell coverage, a secondary carrier from

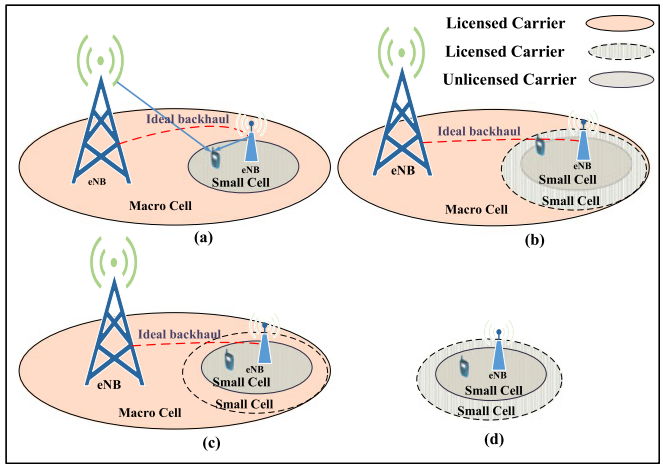


Fig. 3. Operation scenarios of LAA [3].

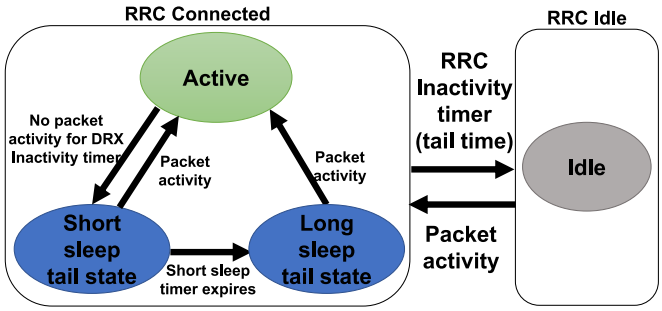


Fig. 4. RRC states in LTE.

unlicensed band could be used for data exchange. This deployment scenario requires idle backhaul between macro and small cells.

- Fig. 3b depicts the usage of different licensed carriers for macro cells and small cells. The different licensed carrier requirement limits the applicability.
- Fig. 3c illustrates the usage of same licensed carriers for macro cells and small cells. The same licensed carrier for both macro cells and small cells might require detailed scheduling and synchronization.
- The licensed carrier and unlicensed carrier for a small cell without any macro cell coverage are delineated in Fig. 3d.

*Radio Access of LAA.* For LAA radio access, mobile UE needs to perform CCA. European Telecommunication Standards Institute defines two types of CCA schemes: Frame Base Equipment (FBE) and Load Base Equipment (LBE) CCA schemes [24]. (i) In FBE, a frame base equipment is used to perform CCA by using energy detection. If the transmitter observes that energy level on the selected channel is lower than a predefined threshold, the channel is considered idle. The transmitter now can start the transmission for MCOT. Otherwise, if the channel is busy, the transmitter waits for a fixed amount of time and performs CCA again. Upon successful reception of the packet, the equipment skips the CCA and immediately transmits the acknowledgment packet. (ii) In LBE, CCA is performed in a similar way as FBE, before starting the transmission. If the transmitter finds that the channel is idle, it can transmit for MCOT. However, if the medium is busy, the transmitter performs Extended CCA (ECCA). In ECCA the channel is observed for the duration of $N \times CCA$ observation time. The value of $N$ is randomly chosen from $\{1, \quad q\}$, where $q$ is a fixed in the range $\{4, \quad 32\}$ [3].

## 2.2 LTE DRX

The UE's Physical Downlink Control Channel Activity monitoring activity is controlled by configuring the DRX mechanism with Radio Resource Control (RRC). An LTE device is either in RRC Connected state or in RRC Idle state after switching on the devices [9], [14]. As shown in Fig. 4, UE transits between two states based on the traffic activity. LTE DRX could be configured in both RRC Connected and RRC Idle states [9], [12]. However, the configuration parameters and functionality are different for these two states. Since data transmission takes place during the connected state, we focus on RRC Connected state DRX and summarized as follows:

- During the RRC Connected state, DRX allows UE to transit between active and tail states (short and long sleep state).

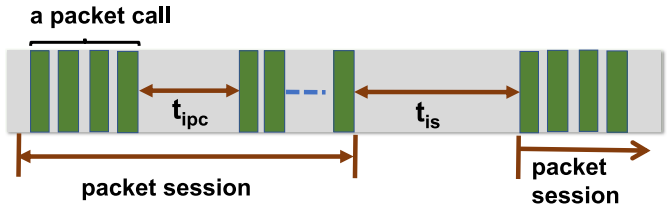


Fig. 5. ETSI traffic model [17].

- UE wakes up after every short/long sleep state and monitors the PDCCH, to check if there is any transmission over the shared data channel allocated to this UE. If there is no packet activity, UE again switches back to the sleep state; otherwise, on the arrival of a packet, UE transits to the active state, serves the packet and remains in that state until the inactivity timer expires. The inactivity timer restarts if another packet arrives before its expiry. UE shifts to short sleep state after the expiry of the inactivity timer. After the expiry of short sleep timer, if there is no packet in the buffer, UE switches to long sleep state.
- In RRC Connected state, if there is no packet for RRC inactivity timer (tail time), the network releases the connection and UE switches to RRC Idle state [13].
- During the Idle state, UE consumes minimum battery power and transits back to RRC Connected state on a packet arrival.
- The DRX is configured by parameters, like inactivity timer, ON duration, short sleep duration and long sleep duration [9].

## 2.3 Traffic Models

Data traffic patterns over Internet are often self-similar and modeled by heavy-tailed distributions, like Pareto and Weibull distributions [25]. We consider ETSI traffic model for our analysis [17], which recommends packet transmission time and packet size to follow truncated Pareto distribution. As shown in Fig. 5, wireless data traffic usually consists of several sessions, with intersession arrival time $t_{is}$. Depending on the application, each session might consist of one or multiple packet calls, e.g., web surfing consists of a sequence of packet calls during one session and video streaming usually consists of one packet call for each session [14], [25]. The major parameters of ETSI traffic model are as follows:

- *Session inter-arrival time* ($t_{is}$)-modeled as an exponential distribution with mean $1/\lambda_{is}$.
- *Packet inter-arrival time* ($t_{ip}$)-drawn from an exponential distribution with mean $1/\lambda_{ip}$.
- *Number of packet calls per session* ($N_{pc}$)-assumed to be a geometric distribution with mean $\overline{n}_{pc}$.
- *Packet call inter-arrival time* ($t_{ipc}$)-modeled as an exponential distribution with mean $1/\lambda_{ipc}$.
- *Number of packets per packet call* ($N_p$)-obeys geometric distribution with mean $\overline{n}_p$.

According to ETSI model, at any time instant the next packet call belongs to a new session or ongoing session with probabilities $P_{ns}$ and $P_{os}$ respectively. Since $N_{pc}$, the number of packet call during each session has a geometric distribution, therefore $P_{ns} = 1/\overline{n}_{pc}$ and $P_{os} = 1 - 1/\overline{n}_{pc}$.

TABLE 2
Idle Period Parameters for the Generalized Pareto Distribution [15]

| Load | Duty Cycle | Idle Period | | |
|---|---|---|---|---|
| | | $\mu$ | $\sigma$ | $\xi$ |
| Very low | 0.09 | 3.6100 | 38.3633 | 0.2125 |
| Low | 0.29 | 3.5780 | 10.9356 | 0.1784 |
| Medium | 0.51 | 3.5160 | 4.6583 | 0.2156 |
| High | 0.71 | 3.5310 | 2.6272 | 0.2119 |
| Very High | 0.93 | 3.5160 | 1.6609 | 0.0068 |

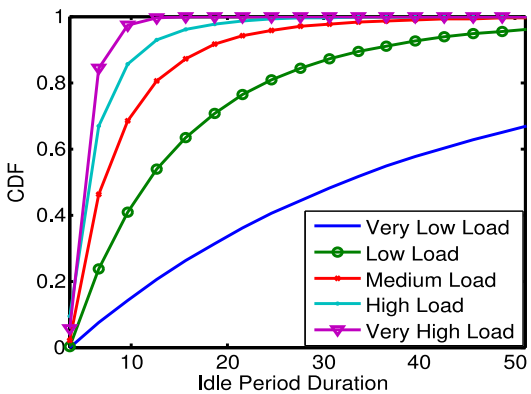


Fig. 6. Empirical distribution of idle periods for different load.

### 2.4 Channel Access Mechanism

LAA adopts LBT process to access the unlicensed spectrum. The spectrum occupancy model for Dynamic Spectrum Access (DSA)/Cognitive Radio (CR) has been already explored[26]. Channel holding time for WLAN channel has been studied in [27]. Unlike continuous-time Markov chain (CTMC), the state holding time does not follow an exponential distribution, but generalized Pareto distribution [27]. The work in [16] characterizes the idle channel period using generalized Pareto distribution for a different types of channel load. In [15] the channel occupancy pattern is modeled by continuous time semi-Markov chain (CTSMC), where the state holding time could follow any arbitrary distribution. The sojourn time or state holding time could be modeled at long timescale using generalized Pareto distribution. Using [15], [16] the probability of channel idle time $\Omega(t_{idle})$ is given as

$$\Omega(t_{idle}) = \frac{1}{\sigma}\left(1 + \frac{\xi(t_{idle} - \mu)}{\sigma}\right)^{\left(-\frac{1}{\xi}-1\right)}, \quad (1)$$

where location $\mu$, shape $\xi$ and scale $\sigma$ for the different traffic load conditions are given in Table 2 [15]. The values shown for location parameter $\mu$ are determined by the time resolution of the spectrum analyzer and could be tailored to the particular scenario under study [15]. Using Equation (1) and Table 2, Fig. 6 demonstrates the probability distribution of idle channel for the different channel load. For low load, the probability of channel availability is high over a long duration. On the other hand, at high load conditions, the probability of channel availability is quite low. For LAA channel idle time modeling, we consider the same generalized Pareto distribution, given in Equation (1).

TABLE 3
List of Symbols and Acronyms Used

| Sym. | Description | Acronym | Expansion |
|---|---|---|---|
| $t_{ser}$ | Packet serving time | LAA | Licensed Assisted Access |
| $t_i$ | Inactivity Timer | DRX | Discontinuous Reception |
| $n_i$ | Maximum number of Inactivity Timer | PDCCH | Physical Downlink Control Channel |
| $t_{on}$ | On duration | LBT | Listen Before Talk |
| $n_{on}$ | Maximum number of ON duration | CCA | Clear Channel Assessment |
| $t_{ss}$ | short sleep timer | MCOT | Maximum Channel Occupancy Time |
| $t_{laa}$ | LAA sleep timer | FBE | Frame Based Equipment |
| $P_{lm}$ | Prob[State transition] | LBE | Load Base Equipment |
| $\phi_k$ | Steady state Probability | ETSI | European Telecom. Standards Institute |
| $\zeta$ | Prob[Interference] | RRC | Radio Resource Control |

As conventional DRX does not consider the channel access mechanism and MCOT, it is not suitable for LTE operation in the unlicensed band. This motivates us to redesign the DRX for the operation of LTE in unlicensed band. We (a) model the DRX for LAA LTE; (b) analyze the resource usage in LAA-DRX; (c) demonstrate the power saving gain with nominal delay cost.

## 3 LAA-DRX Mechanism

In this section, we first present LAA-DRX proposal. We then analytically compute the power saving factor, wake up latency and optimum resource usage in LAA-DRX. Table 3 lists major notations used in this paper.

### 3.1 Our Proposal

We model LAA-DRX mechanism as a semi-Markov model. The semi-Markov process is general, where one can predict the future possible state based on the current state object. The semi-Markov process model is used, as the time between state transition and holding time (sojourn time) of states are random variables [28]. Moreover, semi-Markov process model does not possess memoryless property, if the sojourn time is not exponentially distributed. States $S_1$ is an active state, $S_2$ short sleep state, $S_3$ is ON state and $S_4$ is LAA sleep state respectively. Fig. 7 delineates the state transition dynamics, where $P_{lm}\ \forall\ l, m\ \epsilon\ \{1, 2, 3, 4\}$ are the transition probabilities from state $l$ to $m$. Since there is no guarantee of channel availability, the channel occupancy time is limited for LAA. Naturally, either LAA-DRX sleep timer should be short, or the ON duration should be long enough to allow a feasible time for the UE to obtain channel access [3]. Based on the state model in Fig. 7, UE could be in one of the following four states:

(1) *Active State* ($\mathbf{S_1}$)*:* In active state, UE consumes maximum power to transmit/receive the packet and/or monitor the PDCCH. During this state, arrival of a packet before the expiry of $t_i$, restarts the inactivity timer. If inactivity timer expires before the next packet arrival, UE transits to the Short Sleep state $S_2$. For a fair coexistence of LTE and WiFi, the maximum packet serving time should not exceed the MCOT. To limit the packet serving time $t_{ser}$, we first set a very

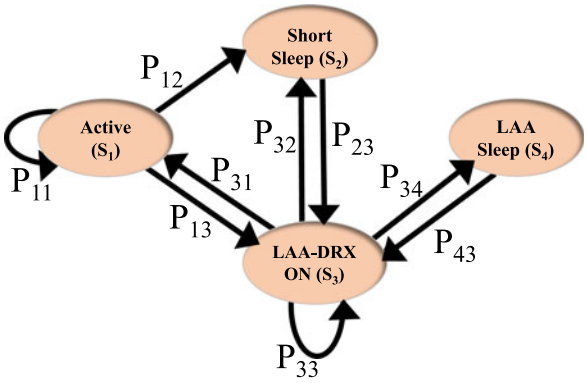


Fig. 7. LAA-DRX states: Semi-Markov process model.

small value of $t_{ser}$. The value of $t_{ser}$ is increased at every restart of the inactivity timer $t_i$. The inactivity timer $t_i$ repeats $n_i$ times, such that $t_{ser} + n_i t_i$ = MCOT. After occupying the unlicensed channel for MCOT, if packets are remaining in the buffer, the UE switches to the ON state $S_3$ for obtaining access to the unlicensed channel again.

(2) *Short Sleep State* (**$S_2$**)*:* The expiry of inactivity timer ($t_i$) before the next packet arrival makes the UE transits from active to the short sleep state with probability $P_{12}$. In $S_2$, UE neither transmits/receives nor monitors PDCCH. The UE remains in this state for short sleep time $t_{ss}$ and saves the power. At the expiry of short sleep timer $t_{ss}$, UE returns back to the ON state ($S_3$) with probability $P_{23}$.

(3) *LAA-DRX ON State* (**$S_3$**)*:* In state $S_3$, UE receives an indication of the packet arrival and channel availability of unlicensed band over the licensed channel. If UE receives an intimation of the packet arrival and the unlicensed channel is also idle, UE transits to active state $S_1$. During this state, if there is no packet activity or channel is not available, UE returns back to short sleep state $S_2$. In $S_3$, if a packet has arrived, but the channel is not available, eNB can extend the ON period of UE by $n_{on}$ number of times. If eNB has knowledge of channel availability, it makes the UE switch to LAA sleep state $S_4$ with probability $P_{34}$, as shown in Fig. 7.

(4) *LAA Sleep State* (**$S_4$**)*:* In $S_4$ state, UE neither transmits/receives nor monitors the PDCCH. UE remains in this state for the time equal to $t_{laa}$ and after the expiry of LAA sleep time, UE transits back to ON state $S_3$, with probability $P_{43}$. The LAA sleep time $t_{laa}$ is not fixed, but variable.

Since licensed channel circuitry and unlicensed channel circuitry work separately, the licensed circuitry also needs to undergo DRX for power saving. Hence, small DRX ON period of licensed and unlicensed channel needs to be aligned to enable the communication between the licensed and unlicensed channel. As delineated in Fig. 8, UE can switch from ON state $S_3$ to active state $S_1$ or Short/LAA sleep states ($S_2/S_4$), based on packet arrival and unlicensed channel intimation during the ON period. It is observed from Fig. 8 that UE can transit from active state $S_1$ to short sleep state $S_2$, if there is no packet remaining in the buffer. UE can also switch from $S_1$ to $S_3$, if packets are remaining in the buffer after MCOT. The LAA-DRX flow diagram is presented in Fig. 9, for communication between eNB, UE and LAA small cell (LAA SCell). The entire procedure is enumerated as follows:

(1) LAA-DRX is negotiated between UE, corresponding eNB and LAA SCell.
(2) eNB senses the unlicensed channel during the ON period and intimates to UE over the licensed channel.
(3) If the unlicensed channel is available, UE transmits/receives the data over the unlicensed channel for allowed MCOT.
(4) At expiry of MCOT, if packets are remaining in the buffer, eNB again senses the unlicensed channel and intimates to UE over the licensed channel.
(5) After transmitting/receiving the packets, UE negotiates the DRX and switch to short sleep state $S_2$.
(6) eNB senses the unlicensed channel during the ON period. If unlicensed channel is not available, eNB might extend the ON period [29]. If eNB does not get access to unlicensed channel, based on the knowledge of unlicensed channel, eNB transits UE to Short/LAA sleep state.

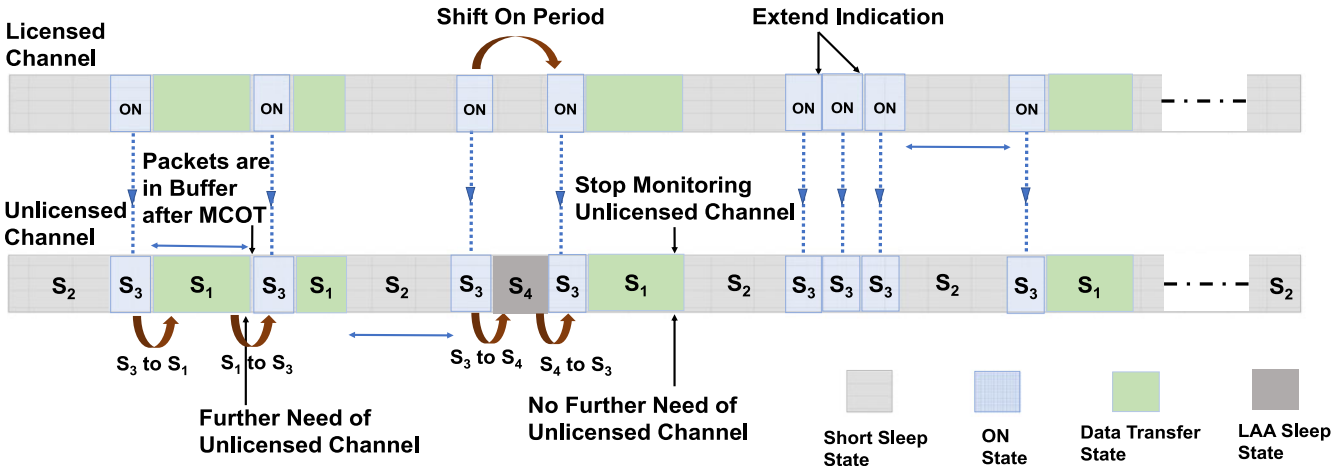


Fig. 8. Synchronization between licensed channel and unlicensed channel.

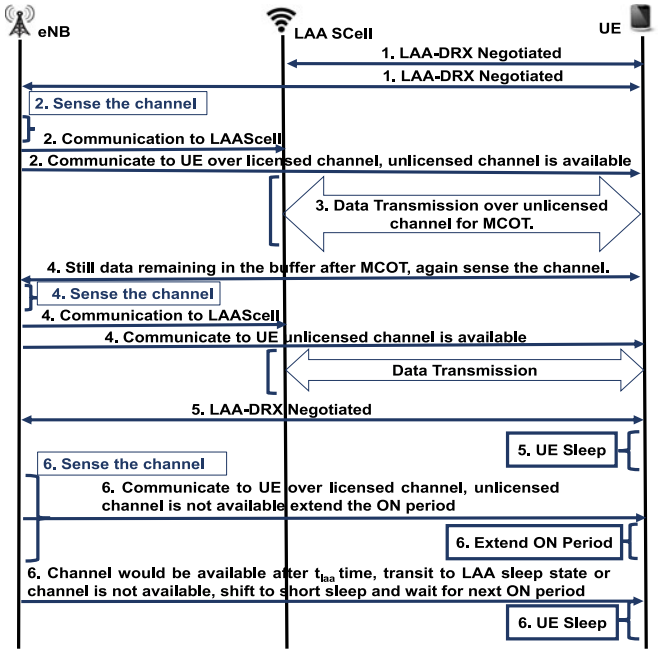


Fig. 9. LAA-DRX: Message flow diagram.

### 3.2 Power Saving and Wake Up Latency Analysis

In this section, we estimate the performance parameters by estimating the steady state probability and holding time in different states.

*Steady State Probability Estimation.* Observing Fig. 7, at the time of state transitions, we could obtain an embedded Markov chain. When UE is in state $S_1$, if no packet arrives before the expiry of inactivity timer, UE transits to state $S_2$ with probability $P_{12}$. Otherwise, on arrival of a new packet, UE continues to stay in the same state $S_1$, with probability $P_{11}$. After $n_i$ number of inactivity time intervals $t_i$ ($t_{ser} + n_i t_i$ = MCOT), if buffer is not empty, UE transits to ON state ($S_3$), with probability $P_{13}$ to access the unlicensed channel again. Based on this discussion the state transition probabilities $P_{11}$, $P_{12}$ and $P_{13}$ are estimated as:

$$\begin{aligned} P_{11} &= P_{os}(t_{ipc} < t_{ser})(t_{ipc} < n_i t_i) + P_{ns}(t_{is} < t_{ser})(t_{is} < n_i t_i) \\ &= P_{os}(1 - e^{-\lambda_{ipc} t_{ser}})(1 - e^{-\lambda_{ipc} n_i t_i}) + P_{ns}(1 - e^{-\lambda_{is} t_{ser}}) \\ &\quad (1 - e^{-\lambda_{is} n_i t_i}) \end{aligned} \tag{2}$$

$$P_{12} = P_{os} e^{-\lambda_{ipc} t_{ser}} e^{-\lambda_{ipc} n_i t_i} + P_{ns} e^{-\lambda_{is} t_{ser}} e^{-\lambda_{is} n_i t_i} \tag{3}$$

$$P_{13} = P_{os}(1 - e^{-\lambda_{ipc} n_i t_i}) + P_{ns}(1 - e^{-\lambda_{is} n_i t_i}). \tag{4}$$

In state $S_2$, UE sleeps for the duration specified in short sleep timer. After expiry of short sleep timer $t_{ss}$, UE transits from $S_2$ to $S_3$, with probability $P_{23} = 1$. In state $S_3$, UE checks for unlicensed spectrum and packet activity. There are four possible state transition probabilities at state $S_3$:

(i) If there is packet activity and the unlicensed channel is available, UE transits to active state $S_1$ with probability $P_{31}$.

(ii) If eNB has no information about the unlicensed channel availability, eNB can extend UE's ON period. The UE extends ON period with probability $P_{33}$. After $n_{on}$ number of ON period, if the channel is not available, UE transits to the short sleep state and waits for next ON Period.

(iii) On the other hand, if there is a packet activity, but unlicensed channel is not available and eNB has information about the next available time of unlicensed channel, UE switches to state $S_4$, with probability $P_{34}$.

(iv) If either there is no packet activity or there is packet activity, but unlicensed channel is not available, the UE goes back to short sleep state $S_2$, with probability $P_{32}$.

Hence, the state transition probabilities are computed as

$$\begin{aligned} P_{31} &= P_{os}(t_{ipc} < t_{on})\Omega + P_{ns}(t_{is} < t_{on})\Omega \\ &= P_{os}(1 - e^{-\lambda_{ipc} t_{on}})\Omega + P_{ns}(1 - e^{-\lambda_{is} t_{on}})\Omega \end{aligned} \tag{5}$$

$$\begin{aligned} P_{33} &= P_{os}(1 - e^{-\lambda_{ipc} n_{on} t_{on}})(1 - \Omega)(1 - \omega) + P_{ns} \\ &\quad (1 - e^{-\lambda_{is} n_{on} t_{on}})(1 - \Omega)(1 - \omega) \end{aligned} \tag{6}$$

$$\begin{aligned} P_{34} &= P_{os}(1 - e^{-\lambda_{ipc} t_{on}})(1 - \Omega)\omega + P_{ns}(1 - e^{-\lambda_{is} t_{on}})(1 - \Omega)\omega \\ P_{32} &= 1 - P_{31} - P_{33} - P_{34}, \end{aligned} \tag{7}$$

where $\Omega$ is the channel idle probability, obtained using Equation (1) and $\omega$ is the probability that eNB has knowledge about the unlicensed channel availability. Since unlicensed channel is used by WiFi and other operators, it is equally likely that eNB has some knowledge about the unlicensed channels. So, we have assumed $\omega$ to follow uniform random distribution. In 802.11, after listening to the wireless medium, mobile stations set their Network Allocation Vector (NAV) by reading the duration field in MAC layer frame headers. NAV is an indicator for a station, about deferred time from accessing the medium [21]. Similarly, during the ON period, eNB needs to use licensed channels to notify the UE about switching into LAA sleep state ($S_4$) for deferred transmission time $t_{laa}$. After the expiry of LAA sleep timer ($t_{laa}$), UE moves to the state $S_3$ with probability $P_{43} = 1$. The state transition probability matrix corresponding to Fig. 7 can be expressed as

$$P = \begin{bmatrix} P_{11} & P_{12} & P_{13} & 0 \\ 0 & 0 & P_{23} & 0 \\ P_{31} & P_{32} & P_{33} & P_{34} \\ 0 & 0 & P_{43} & 0 \end{bmatrix}. \tag{8}$$

The steady state probability $\phi_k$ of any state $S_k$, $\forall k \in \{1, 2, 3, 4\}$, could be obtained by using $\sum_{k=1}^{4} \phi_k = 1$ and the balance equation: $\phi_k = \sum_{l=1}^{4} \phi_l P_{lk}$

$$\Phi = \begin{cases} \phi_1 = & \frac{P_{31}}{P_{31}(1+P_{12})+(1-P_{11})[1+P_{32}+P_{34}]} \\ \phi_2 = & \frac{P_{31}P_{12}+P_{32}(1-P_{11})}{P_{31}(1+P_{12})+(1-P_{11})[1+P_{32}+P_{34}]} \\ \phi_3 = & \frac{(1-P_{11})}{P_{31}(1+P_{12})+(1-P_{11})[1+P_{32}+P_{34}]} \\ \phi_4 = & \frac{P_{34}(1-P_{11})}{P_{31}(1+P_{12})+(1-P_{11})[1+P_{32}+P_{34}]}. \end{cases} \tag{9}$$

*Holding Time Estimations.* After calculating the steady state probabilities, we evaluate the holding time for different states. Let $\varphi_k$, $\forall\, k \in \{1, 2, 3, 4\}$, represent the holding time of any state $S_k$. The computation of expected value of holding time $E[\varphi_k]$ of various states is as follows:

*Holding Time of Active State ($S_1$).* UE enters the state $S_1$ after a packet call, if the unlicensed channel is available. In state $S_1$, UE serves the buffered packets and waits for inactivity timer ($t_i$) to expire. UE leaves the state $S_1$, if no new packet call starts before the expiry of inactivity time. The limitation of MCOT (10 ms), mandates a small value to set the service timer $t_{ser}$. After the expiry of $t_{ser}$, if packets are remaining in the buffer, the value of $t_{ser}$ is increased by $t_i$. The inactivity timer $t_i$ repeats for $n_i$ times. The values of $t_{ser}$, $t_i$ and $n_i$ are selected, such that it should not exceed the limit of MCOT. The holding time of active state $S_1$ is estimated as the sum of the service time $t_{ser}$ and average time duration of inactivity timer $\overline{T}_{t_i}$. The holding time of state $S_1$, $E[\varphi_1]$ is given in Appendix, which can be found on the Computer Society Digital Library at http://doi.ieeecomputersociety.org/10.1109/TMC.2018.2835443.

*Holding Time of Short Sleep State ($S_2$).* The UE remains in short sleep state $S_2$ for time $t_{ss}$ and if any packet arrives during this period, the packet is buffered at LAA SCell until next active period. The holding time for state $S_2$, $E[\varphi_2]$ could be computed as $E[\varphi_2] = t_{ss}$.

*Holding Time of LAA-DRX ON State ($S_3$).* From short sleep state $S_2$ or LAA sleep state $S_4$, UE might transit to ON state $S_3$. In state $S_3$, UE waits for $t_{on}$ period. After $t_{on}$, UE might move to active state $S_1$, if an intimation of packet arrival and unlicensed channel availability is received during $t_{on}$. If a packet has arrived, but the unlicensed channel is not available and eNB has knowledge about the availability time of unlicensed channel, UE might transit to LAA sleep state $S_4$. On packet arrival, if eNB has no knowledge about unlicensed channel availability, eNB can also extend the ON period to preset $n_{on}$ times. If eNB is not able to get the unlicensed channel after $n_{on}$ periods, UE transits to short sleep state $S_2$ and waits for the next ON period. The holding time of state $S_3$, $E[\varphi_3]$ is given in Appendix, available in the online supplemental material.

*Holding Time of LAA Sleep State ($S_4$).* UE remains in state $S_4$ for $t_{laa}$ time. The holding time of state $S_4$, $E[\varphi_4]$ is also shown in Appendix, available in the online supplemental material.

*Performance Parameters.* After calculating $\phi_m$ and $E[\varphi_m]$, $\forall m \in \{1,2,3,4\}$, we estimate the fraction of time UE spends in short sleep state $p_{sc}$, ON state $p_{on}$ and LAA sleeping state $p_{laa}$ as

$$p_{sc} = \frac{\phi_2 E[\varphi_2]}{\phi_1 E[\varphi_1] + \phi_2 E[\varphi_2] + \phi_3 E[\varphi_3] + \phi_4 E[\varphi_4]} \tag{10}$$

$$p_{on} = \frac{\phi_3 E[\varphi_3]}{\phi_1 E[\varphi_1] + \phi_2 E[\varphi_2] + \phi_3 E[\varphi_3] + \phi_4 E[\varphi_4]} \tag{11}$$

$$p_{laa} = \frac{\phi_4 E[\varphi_4]}{\phi_1 E[\varphi_1] + \phi_2 E[\varphi_2] + \phi_3 E[\varphi_3] + \phi_4 E[\varphi_4]}. \tag{12}$$

Using Equations (10), (11), and (12), we can obtain the expression for performance parameters, like power saving factor and wake up latency. The power saving factor $\mu_{sleep}$ is defined as the percentage of the time UE spends in sleep mode (short sleep and LAA sleep state). The power saving factor $\mu_{sleep}$ can be expressed as

$$\mu_{sleep} = p_{sc} + p_{laa}. \tag{13}$$

The power consumed by UE in various states is different. There is a significant difference in the power consumption during an effective data transfer, during the period in which inactivity timer runs while looking for data, during ON duration and during sleep mode [10], [30]. Let $PW_t$, $PW_i$, $PW_{sleep}$, $PW_{on}$ be the energy consumption during the data transmission, inactivity timer run, sleep and ON states respectively. Using the concepts, given in [30], [31] the average power consumption ($E[PW_{cons}]$) due to LAA-DRX could be estimated as

$$E[PW_{cons}] = \frac{\phi_1[PW_t(E[\varphi_1] - t_i) + PW_i\overline{T}_{t_i}]}{\phi_1 E[\varphi_1] + \phi_2 E[\varphi_2] + \phi_3 E[\varphi_3] + \phi_4 E[\varphi_4]} + PW_{sleep}p_{sc} + PW_{on}p_{on} + PW_{sleep}p_{laa}. \tag{14}$$

This power saving is achieved by DRX at the cost of additional delay [11]. The packets arriving during the short sleep state, ON state and LAA sleep state, are buffered at LAA SCell and delivered only when UE returns to an active state. Since inter-packet call idle time and inter-session idle time are exponential distributed random variable, the arrival events are random observers to the sleep duration and ON period [32]. Therefore, average wake up delay caused by short sleep, ON state and LAA sleep is $\overline{t}_{ss} = \frac{t_{ss}}{2}$, $\overline{t}_{on} = \frac{t_{on}}{2}$ $and$ $\overline{t}_{laa} = \frac{t_{laa}}{2}$ respectively. The overall wake up latency $\delta$ is given as

$$\delta = p_{sc}\overline{t}_{ss} + p_{on}\overline{t}_{on} + p_{laa}\overline{t}_{laa}. \tag{15}$$

Using Equations (13), (14), and (15), we can obtain the dynamics of power saving factor, power consumption and wake up latency trade-off.

### 3.3 Optimum Resource Usage in LAA-DRX

DRX is used to save the UE's power consumption by periodically turning off the radio circuitry. The eNB has DRX parameters of each UE and allocates the resources to UE only during the wake up state. The resources available during the sleep period could be assigned to other devices/equipment. For example, $\alpha$ UEs had established the RRC connection with eNB and out of which $\alpha_1$ UEs are actively transmitting the packets at any given time instant, then resources are allocated based on $\alpha_1$ UEs. In the absence of DRX, resources are allocated based on $\alpha$ UEs [33]. In our proposed LAA-DRX state diagram, shown in Fig. 7, the resources are needed during the active state $S_1$ and ON state $S_3$. Since there is no transmission over the unlicensed channel during states $S_2$ and $S_4$ (off periods), no resource is required during sleep state.

The basic unit for resources assigned in LTE is Resource Block (RB). The RB allocated for transmission/reception are referred as resource batch. For LAA-UE, assigned with a resource batch, the maximum throughput is defined as the probability of the usage of that resource batch without any interference [34]. The interference of WiFi network to LAA network depends upon the channel conditions, traffic generated by WiFi and deployment scenario of WiFi/LAA network. Since all the parameters are independent, we consider the probability of interference occurrence from WiFi at each resource batch having an independent and identical distribution (i.i.d.) $\zeta$. If an UE requests one resource batch and LAA network assign exact one resource batch, the

maximum throughput of that LAA-UE is $(1-\zeta)$. If LAA SCell assigns two resource batches to an UE requesting one resource batch, the usage of two resource batch is $(\frac{1-\zeta^2}{2})$, which is less than the usage of one resource batch. If a LAA-UE is assigned with $K$ resource batches, the LAA-UE experiences a different level of interference from WiFi for the same resource batch. Therefore, for efficient resource usage LAA SCell allocates these resource batches to other LAA-UEs. The optimum number of UEs sharing the resource batch, from a given pool, consists of $K$ resource batches is given by [34]

$$N^*_{UE} = \begin{cases} \frac{K}{1-\zeta^K}, & \text{if } \frac{K}{1-\zeta^K} \text{ isaninteger} \\ \lfloor \frac{K}{1-\zeta^K} \rfloor, & \text{otherwise.} \end{cases} \tag{16}$$

Using the optimum usage [34] of each resource batch, when $N^*_{UE}$ LAA-UEs are sharing K resource batches, the resource batch usage $\rho_1$ during the active state $S_1$ can be obtained as

$$\rho_1 = \begin{cases} \left(1-\frac{1-\zeta^K}{K}\right)^{\frac{K}{1-\zeta^K}-1}, & \text{if } \frac{K}{1-\zeta^K} \text{ is an integer} \\ \lfloor \frac{K}{1-\zeta^K} \rfloor \left(\frac{1-\zeta^K}{K}\right)\left(1-\frac{1-\zeta^K}{K}\right)^{\lfloor \frac{K}{1-\zeta^K} \rfloor -1}, & \text{otherwise.} \end{cases} \tag{17}$$

DRX reduces the PDCCH monitoring activity, thus resulting in less resource usage for control channel. For proposed LAA-DRX (Fig. 7), UE searches for the channel during state $S_3$, after receiving an intimation from eNB. Let, $N_{UE}$ be the number of users and $M$ be the number of resources for the control channel. The probability that an UE is able to get the control channel is $\frac{1}{M}$. Hence, with the probability of WiFi interference $\zeta$, the usage of control channel resources can be obtained by

$$\rho_3 = N_{UE}\left(\frac{1-\zeta}{M}\right). \tag{18}$$

Using Equations (9), (17), and (18), the optimum resource usage ($\rho^*$) in LAA-DRX could be estimated as

$$\begin{aligned} \rho^* &= \phi_1 \times \rho_1 + \phi_3 \times \rho_3 \rho^* \\ &= \left(\frac{P_{31}}{P_{31}(1+P_{12}) + (1-P_{11})[1+P_{32}+P_{34}]}\right) \times \rho_1 \\ &\quad + \left(\frac{(1-P_{11})}{P_{31}(1+P_{12}) + (1-P_{11})[1+P_{32}+P_{34}]}\right) \times \rho_3. \end{aligned} \tag{19}$$

By using Equation (19), we can obtain the resource usage due to LAA-DRX.

## 4 Performance Evaluation

In this section, we evaluate the performance of our proposed model in terms of power saving factor and wake up latency. We also present the comparison of LAA-DRX with LTE DRX mechanism. The simulation of LAA-DRX is performed using Matlab based discrete event simulation model. The simulation model incorporates the real trace obtained from Umass Trace Repository [18].

TABLE 4
LAA-DRX Performance Parameters

| Parameter | Value |
|---|---|
| Sub-frame length (TTI) | 1 ms |
| $[\lambda_{is}, \lambda_{ipc}, \lambda_{ip}]$ [12] | $[1/2000,\ 1/10,\ 10]$ |
| $[\overline{n}_{pc}, \overline{n}_p]$ [12] | $[5,\ 25]$ |
| In-activity Timer ($t_i$) | 2 ms |
| Maximum No. of In-activity Timer ($n_i$) | 4 |
| On Duration ($t_{on}$) | 1 ms |
| Short sleep duration ($t_{ss}$) [14] | $2 \sim 640$ ms |
| LAA sleep duration ($t_{laa}$) | $1 \sim 10$ ms |
| Transmit power on unlicensed band [34] | 20 dBm |
| Transmit power WiFi station [34] | 15 dBm |
| Path loss model [35] | $= 15.3 + \text{a} \times 10\log_{10}(\text{d})$ |
| Licensed, Unlicensed | a = 3.75, a = 5 |
| AWGN noise power | $-174$ dBm/Hz |
| CCA energy detection threshold [34] | $-62$ dBm |
| Resource batch bandwidth [34] | 20 MHz |

### 4.1 Numerical Analysis

We present the numerical results based on semi-Markov model, formulated by Equations (1), (2), (3), (4), (5), (6), (7), (8), (9), (10), (11), (12), (13), (14), (15), (16), (17), (18), and (19). The unlicensed channel access probability for different types of load in the channel is calculated using Equation (1), for channel idle time $t_{idle} = 10$ ms. The value of $\xi,\ \sigma$ and $\mu$ are given in Table 2. The ETSI model traffic parameters, used for analytical computations are: $\overline{n}_{pc} = 5,\ \overline{n}_p = 25, \lambda_{is} = 1/2000,\ \lambda_{ip} = 10$ and $\lambda_{ipc} = 1/10$ [12]. To set the maximum channel access time to 10 ms, we set the initial value of $t_{ser} = 2$ ms. The value of $t_{ser}$ is increased by selecting inactivity timer $t_i = 2$ ms and $n_i = 4$ ($t_{ser} + n_i t_i = 10$ ms). Table 4 outlines list of parameters with values, including transmit power unlicensed band 20 dBm, transmit power of WiFi station 15 dBm, CCA energy detection threshold $-62$ dBm, resource batch bandwidth 20 MHz, etc. [34].

Figs. 10a and 10b demonstrate the power saving factor and wake up latency for short sleep timer $t_{ss}$. The short sleep timer $t_{ss}$ is varied between 10 ms $\sim$ 640 ms for different load in the channel with same arrival rate. As expected, the power saving increases with the increase in the short sleep duration, because UE consumes minimum power during the sleep state. During low load, the power saving factor increases from $55\% \sim 84\%$ with an increase in short sleep timer. This increase in power saving factor is achieved at the cost of additional wake up latency. For low channel load, with an increase in short sleep timer, wake up latency increases from 3 ms to 206 ms. Note that, in Figs. 10a and 10b, as the channel load increases, the power saving factor and wake up latency increase. For very high load conditions on the channel, the power saving factor is between $66\% \sim 98\%$, with delay 3 ms $\sim$ 314 ms. Moreover, very high load in the channel achieves 12.5 percent higher power saving factor as compared to very low load on the channel. This arises from the fact that high load on the channel thwarts the UE from accessing the unlicensed channel. In Fig. 10b, at 160 ms short sleep time, the wake up latency for the medium load is 65 ms, while the wake up latency of

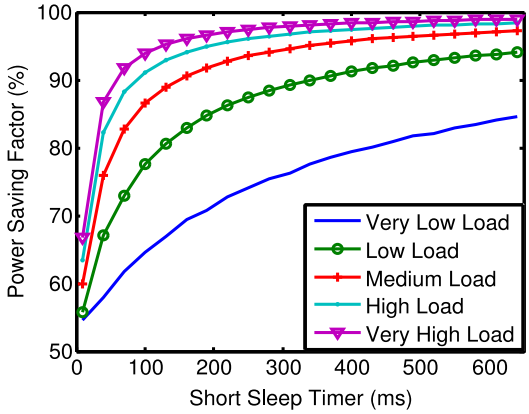


(a) LAA-DRX power saving factor ($\mu_{sleep}$)

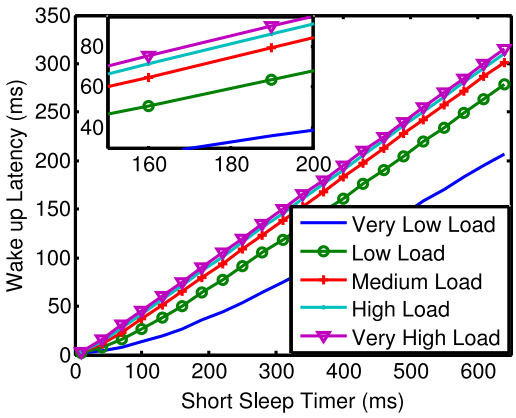


(b) LAA-DRX wake up latency ($\delta$)

Fig. 10. LAA-DRX $\mu_{sleep}$ and $\delta$ under different short sleep timer, for different load and $t_{on} = 1$ ms, $t_{idle} = 10$ ms.

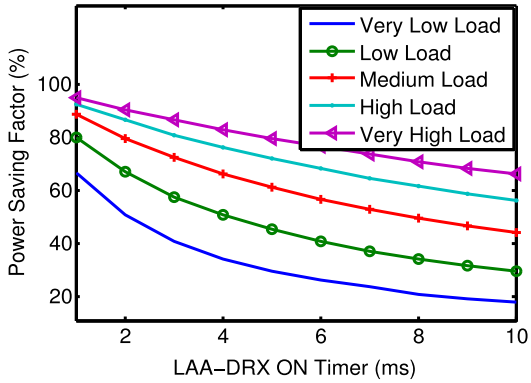


(a) LAA-DRX power saving factor

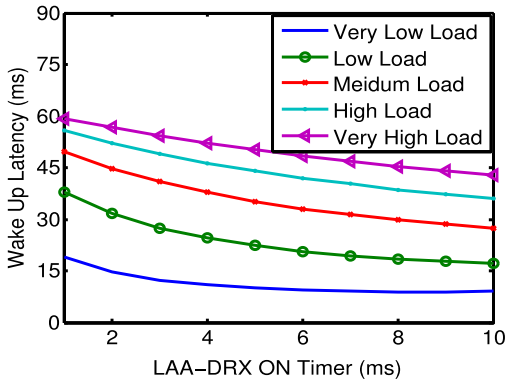


(b) LAA-DRX latency

Fig. 11. LAA-DRX performance under different ON duration, for different load and $t_{ss} = 128$ ms, $t_{idle} = 10$ ms.

very high load is 75 ms. When load increases in the channel, the channel idle probability becomes low as other services occupy the unlicensed channel. The wake up latency of very high load on the channel is on average 9 percent higher than medium channel load.

Figs. 11a and 11b delineate the power saving factor and wake up latency respectively, with varying ON duration, for different channel loads. The figures point out that both the power saving factor and wake up latency decrease with increase in ON duration. Longer ON duration provides more time to the UE to get the unlicensed channel. For very low channel load, almost $17\% \sim 66\%$ power saving and 8.9 ms $\sim 19.1$ ms wake up latency are achieved. The power saving factor and wake up latency increases with increase in the channel load, as higher channel load impedes the UE from accessing the channel. In Figs. 11a and 11b, for very high channel load, almost $66\% \sim 95\%$ power saving and 42.96 ms $\sim 59.27$ ms wake up latency are achieved. The effects of different arrival rates on the power saving factor and wake up latency, for varying short sleep timer are demonstrated in Figs. 12a and 12b. The power saving achieved by arrival rate $\lambda = 0.1$ is 4 percent higher than that of arrival rate $\lambda = 5$. However, it also results in 36 percent increase in delay. As observed from Figs. 12a and 12b power saving factor and wake up latency decreases with increasing arrival rate. The reason lies in the feet that decreasing arrival rate results in faster transition to the short sleep state, which results in longer wake up latency.

Figs. 13a and 13b, illustrate the comparison of LAA-DRX power saving factor and wake up latency with LTE DRX [12]. LTE DRX consists of short and long sleep cycles. As long sleep cycle is not considered in LAA-DRX modeling, we have considered the LTE long sleep cycle timer equal to short sleep cycle timer. In Figs. 13a and 13b the short sleep timer is varied from 1 ms to 640 ms. The power saving factor of LAA-DRX is 4 percent higher than LTE DRX [12]. The corresponding wake up latency of LAA-DRX is 30 ms (on an average) higher compared to LTE DRX [12]. This is because in LAA unlicensed channel is not available all the time, while in LTE licensed channel is dedicated. As observed from Figs. 13a and 13b, at 160 ms short sleep time, LAA-DRX power saving factor is 96 percent with wake up latency of 75 ms, while there is no power saving without DRX. The operation of LAA without DRX would drain the battery, as UE has to keep listening to the network for unlicensed channel/data, even if there is no data or unlicensed channel is not available.

DRX saves UE's power at the cost of an increase in delay. When UE is in the sleep state or unlicensed channel is not available, the packets intended for UE are buffered at eNB until UE returns to active state. This buffering of packets leads to additional delay. Different services have different delay requirements. In LTE network QoS Class Identifier (QCI) is a scalar identifier to describe the traffic characteristics in terms of Packet Delay Budget (PDB) and Packet Loss Rate (PLR). The PDB is the maximum waiting time a packet can tolerate during its delivery between eNB and UE. The standardized QCI characteristics are given in Table 5 [36], [37]. In most non-real-time applications e.g., web browsing,

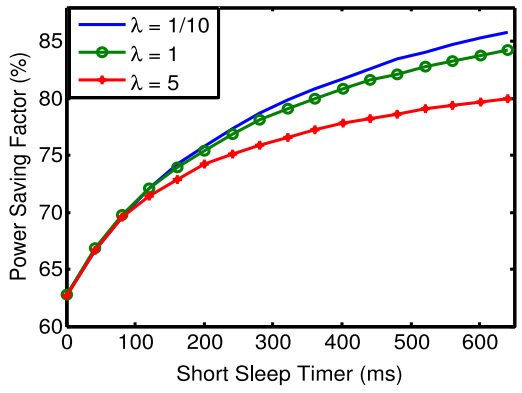


(a) LAA-DRX power saving factor ($\mu_{sleep}$)

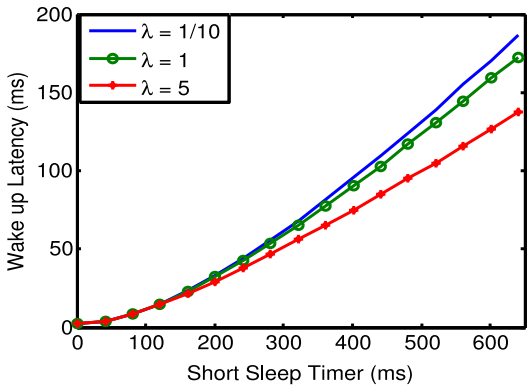


Fig. 12. LAA-DRX $\mu_{sleep}$ and $\delta$ for different arrival rate and $t_{idle} = 10$ ms, $t_{on} = 1$ ms.

email, there is a period of time where UE does not need to monitor the physical downlink control channel continuously [10]. The delay requirement for aforesaid application is relatively high: 300 ms [36], [37]. For such lower-delay-sensitive applications, the network could be configured with a long value of short sleep time, e.g., $t_{ss} = 580$ ms and $t_{on} = 1$ ms (Fig. 13b), for better power saving. However, real-time applications, e.g., voice and video (live streaming), are sensitive to delay [38]. Therefore, for delay sensitive application, delay should be a priority over power saving. For such applications, the network should configured with a small value of short sleep time e.g., $t_{ss} = 190$ ms, $t_{on} = 1$ ms (Fig. 13b). Thus, depending on QCI, the network can select LAA-DRX parameters ($t_{ss}$, $t_{on}$) in such a way, that the delay observed by UE is lower than the required delay. Furthermore, the network may adopt DRX-aware scheduling to optimize the performance [38].

The power consumed by UE during LAA-DRX mode with varying short sleep timer is shown in Fig. 14. During the active state, UE consumes 500 mW for transmission/reception of data and 255.5 mW while inactivity timer runs, not transmitting/receiving any data. The power consumed by UE during the sleep state is 11 mW [10], [30], [31]. During the ON state UE waits for intimation of the unlicensed channel over the licensed channel, the power consumption in this state is 255.5 mW. As observed from Fig. 14, expected power consumption reduces with an increase in short sleep timer as UE consumes minimum power during the sleep state. For very low load conditions on the channel, the power consumption decreases from 99 mW to 45 mW with an increase in short sleep timer. Moreover, the power

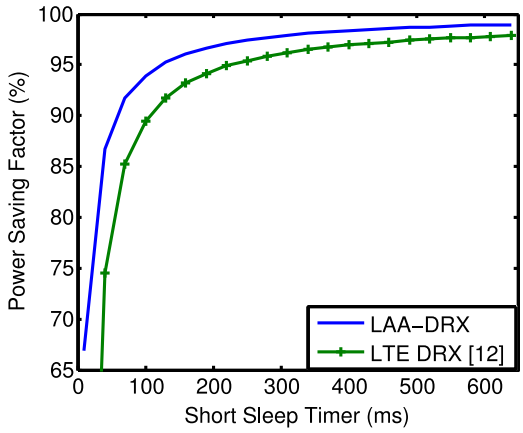


(a) Power saving factor comparison

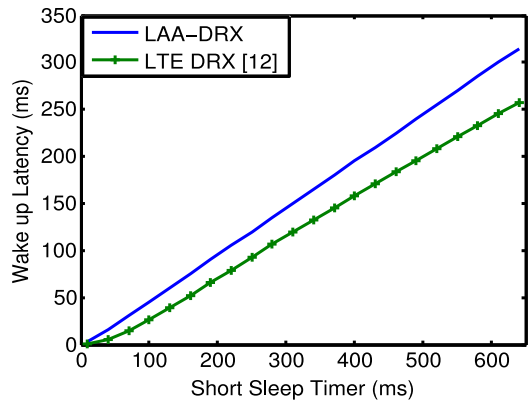


(b) Wake up latency comparison

Fig. 13. LAA-DRX comparison with LTE DRX [12].

consumption of very high load on the channel is 67 percent less than the very low load on the channel. Power consumption is high during very low load on the channel, as UE easily gets the unlicensed channel.

### 4.2 Simulation Using Real Trace

To validate the gain of the proposed LAA-DRX mechanism we perform simulation using Matlab. The simulation setup is explained below:

(1) We assume an LTE macro cell and LAA SCell network with a 20 MHz bandwidth, 120 UEs and 50 WiFi transceivers are randomly and uniformly deployed in the area with an inter-site distance of

TABLE 5
Standardized QCI Characteristics [36], [37]

| QCI | Type | PDB | PLR | Example Services |
|---|---|---|---|---|
| 1 | GBR | 100 ms | $10^{-2}$ | Voice |
| 2 | GBR | 150 ms | $10^{-3}$ | Live Streaming |
| 3 | GBR | 50 ms | $10^{-3}$ | Real Time Gaming |
| 4 | GBR | 300 ms | $10^{-6}$ | Buffered Streaming |
| 5 | Non-GBR | 100 ms | $10^{-6}$ | IMS Signaling |
| 6 | Non-GBR | 300 ms | $10^{-6}$ | TCP-based apps |
| 7 | Non-GBR | 100 ms | $10^{-3}$ | Interactive Gaming |
| 8 | Non-GBR | 300 ms | $10^{-3}$ | TCP-based Video |
| 9 | Non-GBR | 300 ms | $10^{-6}$ | TCP-based Video |

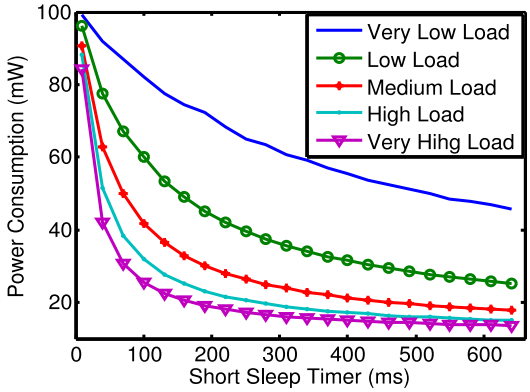


Fig. 14. LAA-DRX Power consumption for different short sleep timer, for different load and $t_{on} = 1$ ms, $t_{idle} = 10$ ms.

TABLE 6
Real Trace Obtained from Umass Trace Repository

| No | Time (s) | Source | Destination | Prot–ocol | Len (B) | Info |
|---|---|---|---|---|---|---|
| 1 | 0.000 | 10.39.72.163 | 95.211.111.66 | UDP | 96 | 4001->3912 Len=52 |
| 2 | 0.137 | 95.211.111.66 | 10.39.72.163 | UDP | 124 | 3912->4001 Len=80 |
| ... | ... | ... | ... | ... | ... | ... |

100 m. The transmission power of LAA is 20 dBm, while the transmission power of WiFi station is 15 dBm [34]. Other parameters for simulation are given in Table 4.

(2) The simulation is fed with "Monitoring Mobile Video Delivery to Android Devices" trace, obtained from Umass Trace Repository [18]. The video streaming trace is used as it is expected by 2,022 over three-quarters of mobile data traffic will be video traffic [1]. UE's power consumption will be high with this class of traffic. Table 6 shows a sample of the trace, collected by Eittenberger et al. [39] in an actual wireless network for both HTTP and peer-to-peer video streaming applications. The measurement is performed in three different settings: (1) The first measurement was performed with mobile during a bus ride of an inner-city route in Bamberg. The maximum speed is 50 km/h and trace length of 3.6 km. (2 $\sim$ 3) Additionally, two stationary measurements performed in the office with 3G and WiFi network. The trace measurement consists of three devices, each including two measurement runs. The trace (Table 6) consist of fields: time in second (packet receiving time), source address, destination address, length (bytes captured) and Info (source & destination port number and data in bytes). We used the packet receiving time from the trace, to generate the packets of size equal to length field in the trace.

(3) We develop discrete-event simulation to implement the LAA-DRX mechanism. Four types of events are considered: (1) packet arrival (2) active (3) sleep and (4) wake up events. The packet arrival event reads the packet generation time and size of data from the data set, given in Table 6 and pushes the packets in the buffer. UE listens for packets information and unlicensed channel intimation, during the wake up event over the licensed channel. After getting the intimation of packets and unlicensed channel availability, UE switches to active event to serve the packets. If unlicensed channel is not available or no packet arrives before inactivity time expires, UE switches to sleep event. During sleep event UE sleeps for short sleep timer ($t_{ss}$) or LAA sleep timer ($t_{laa}$). After the expiry of sleep timer, UE again switches to wake up event.

(4) We use major simulation results, like sleep time, total wake up time, packet arrival time, packet serving time and simulation clock to calculate the power saving factor and latency. Each simulation is executed for 5 minutes and average values are reported.

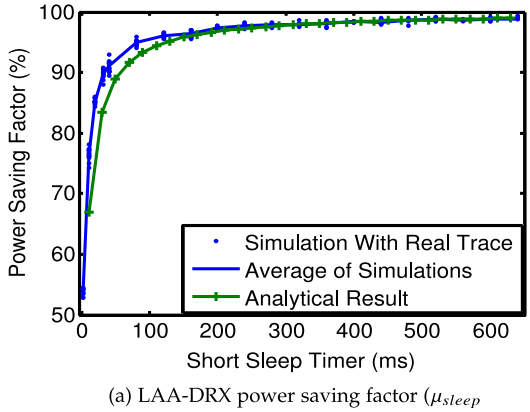


(a) LAA-DRX power saving factor ($\mu_{sleep}$

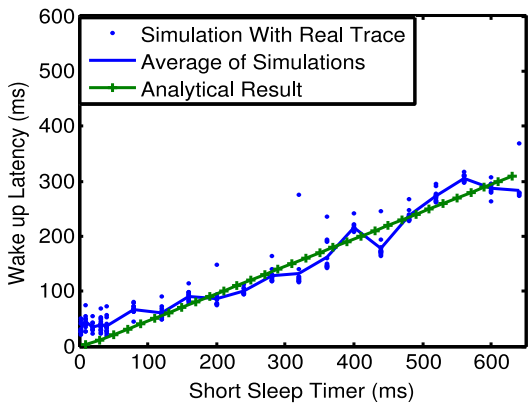


(b) LAA-DRX wake up latency ($\delta$)

Fig. 15. LAA-DRX power saving and wake up latency, analytical and simulation for varying sleep timer.

Figs. 15a and 15b depict the variation of sleep time and wake up delay for varying short sleep timer. The dynamics in power saving, obtained from simulation are 97 percent similar to that analytical model. The power saving factor is between $53\% \sim 98\%$ with 5 ms $\sim$ 307 ms wake up latency. It is noticeable from Fig. 15a that the long value of short sleep time is preferable to increase the power saving factor. For a given MCOT and ON period, a long value of the short sleep time increases the sleep time. However, as depicted in Fig. 15b, wake up latency increases with long value of short sleep time due to longer buffering in each cycle. The power saving factor and wake up latency for varying ON periods are shown in Figs. 16a and 16b. The On timer is varied between $1 \sim 10$ ms, while short sleep timer $t_{ss}$ is kept constant at 64 ms. As observed from Fig. 16a, power saving factor decreases with increase in ON timer because longer ON timer delays the sleep cycle. The Fig. 16b point out that a

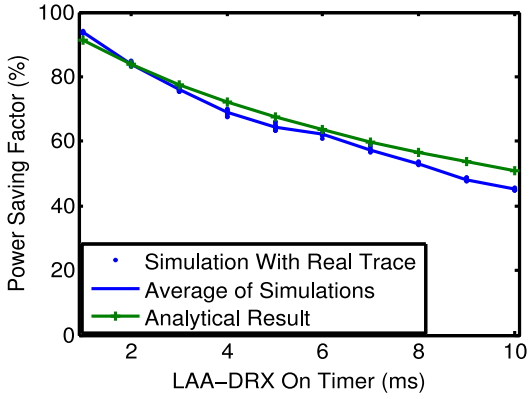


(a) LAA-DRX power saving factor ($\mu_{sleep}$)

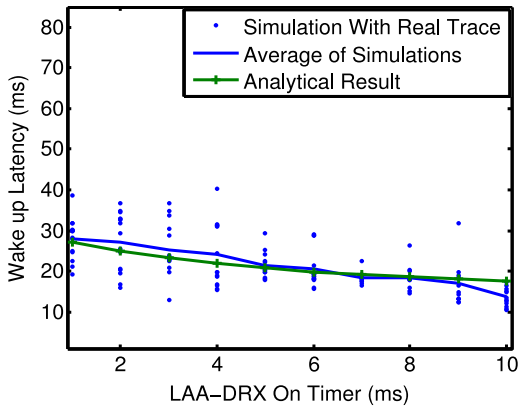


(b) LAA-DRX wake up latency ($\delta$)

Fig. 16. LAA-DRX power saving and wake up latency, analytical, and simulation for varying ON timer.

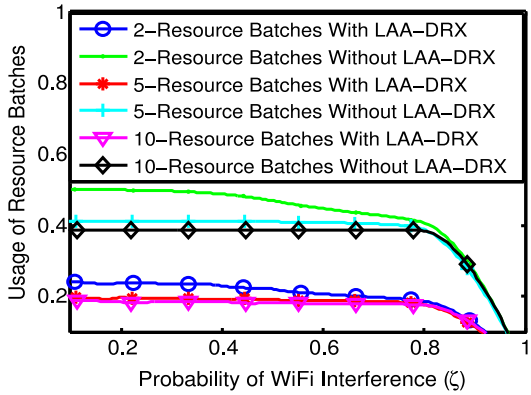


Fig. 17. Usage of resource batches for WiFi interference ($\zeta$).

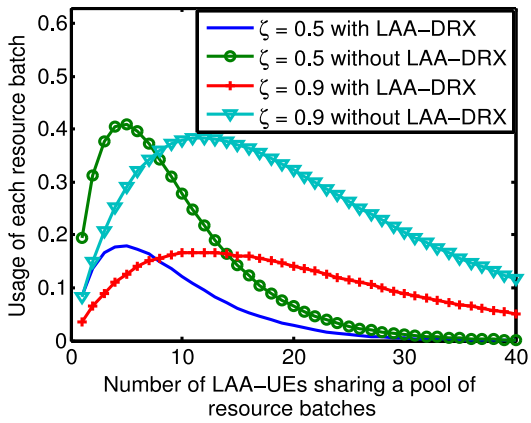


Fig. 18. Usage of resource batches as $N_{UE}$ LAA-UE sharing a pool of five resources batches.

longer ON timer reduces the wake up latency. Moreover, Figs. 16a and 16b presents the comparison between analytical and simulation results. In Fig. 16a the average power saving lies between 45 to 93 percent, which is close to analytical results. The difference between analytical and simulation for power saving is around 4 percent.

Fig. 17 delineates the usage of resource allocated to UE for different probability of WiFi interference with and without LAA-DRX. The usage depends on the WiFi interference. As observed from Fig. 17, the resource usage is quite high for low WiFi interference. The resource usage reduces with increase in WiFi interference, as higher interference thwarts the use of unlicensed channel. Fig. 17 also presents the usage of resource batches for an UE assigned with 2, 5 and 10 resource batches. The usage of 5 resource batches is less than the usage of 2 resource batches, as LAA-UE suffers from different levels of interference for the same resource batch. The resources used with LAA-DRX is 58 percent less, on an average, than the resources used without LAA-DRX. The resource batch usage decreases with LAA-DRX, as UE needs resources during the active state $S_1$ and ON state $S_3$ for transmission/reception of data and control signals. During the sleeping time in states $S_2$ and $S_4$, the resources can be assigned to other UEs.

Fig. 18 shows the usage of resource batches versus the number of LAA-UEs sharing the pool of resource batches with different level of WiFi interference. For WiFi interference level $\zeta = 0.5$, the maximum usage of each resource batch is 40 percent without LAA-DRX and 17 percent with LAA-DRX. The number of UEs sharing resource pool increases with the increase of WiFi interference, as the interference observed by each UE for the same assigned resource batch is different. As observed from Fig. 18, for $\zeta = 0.9$, with a pool of 5 resource batches shared by 11 UEs, maximum usage of 38 percent is achieved without LAA-DRX and 16 percent with LAA-DRX.

## 5 Conclusion

In this paper, we have proposed a novel LAA-DRX process for energy, as well as resource savings for LTE operations in unlicensed band. Our proposed LAA-DRX model enables UE to save power, when unlicensed channel is occupied or there is no data for transmission. The performance of our proposal, in terms of power savings factor and wake up latency, is analyzed by using a new four state semi-Markov model. Performance analysis and simulation results, demonstrate that comparing to LTE DRX, our proposed LAA-DRX achieves 4 percent more power saving at the cost of 30 ms wake up latency. Moreover, comparing to LAA operations without DRX, it also reduces the OFDMA resource usage by almost 58 percent.

## Acknowledgments

This research was supported by the Basic Science Research Program through the National Research Foundation of Korea (NRF) funded by the Ministry of Education (NRF-2016R1D1A1B03935633).

## REFERENCES


[1] P. Cerwall, et al., "Ericsson mobility report," Jun. 2017. [Online]. Available: https://www.ericsson.com/assets/local/mobility-report/documents/2017/ericsson-mobility-report-june-2017.pdf

[2] H. J. Kwoon, et al., "Licensed-Assisted access to unlicensed spectrum in LTE release 13," *IEEE Commun. Mag.*, vol. 55, no. 2, pp. 201–207, Feb. 2017.

[3] 3GPP TR 36.889, "Study on licensed-assisted access to unlicensed spectrum," *Rel.13, V13.0.0*, Jun. 2015.

[4] B. Chen, et al., "Coexistence of LTE-LAA and Wi-Fi on 5 GHz with corresponding deployment scenarios: A survey," *IEEE Commun. Surv. Tut.*, vol. 19, no. 1, pp. 7–32, Jan.–Mar. 2017.

[5] L. Sun "The unlicensed spectrum usage for future IMT technologies," *Int. Workshop-Vis. Technol. 5G*, Seoul, Korea, Sep. 2013.

[6] 3GPP TSG-RAN Meeting # 65, Agenda item: 14.1.1, "Study on licensed-assisted access using LTE," *3GPP RP-141664*, Edinburgh, Scotland, Sep. 2014.

[7] A. Babaei, et al., "On the impact of LTE-U on Wi-Fi performance," *Int. J. Wireless Inf. Netw.*, vol. 22, no. 4, pp. 336–344, 2015.

[8] Y. Song, et al., "Coexistence of Wi-Fi and cellular with listen-before-talk in unlicensed spectrum," *IEEE Commun. Lett.*, vol. 20, no. 1, pp. 161–164, Jan. 2016.

[9] 3GPP TS 36.331, "Evolved universal terrestrial radio access (E-UTRA); Radio Resource Control (RRC); protocol specification," *Rel. 14, V.14.4.0*, Sep. 2017.

[10] C. C. Tseng, et al., "Delay and power consumption in LTE/LTE-A DRX mechanism with mixed short and long cycles," *IEEE Trans. Veh. Technol.*, vol. 65, no. 3, pp. 1721–1734, Mar. 2016.

[11] K. Zhou, et al., "LTE/LTE-A discontinuous reception modeling for machine type communications," *IEEE Wireless Commun. Lett.*, vol. 2, no. 1, pp. 102–105, Feb. 2013.

[12] S. Fowler, et al., "Analytical evaluation of extended DRX with additional active cycles for light traffic," *Comput. Netw.*, vol. 77, pp. 90–102, 2015.

[13] J. Huang, et al., "A close examination of performance and power characteristics of 4G LTE networks," in *Proc. 10th Int. Conf. Mobile Syst. Appl. Serv.*, 2012, pp. 225–238.

[14] A. T. Koc, et al., "Device power saving and latency optimization in LTE-A networks through DRX configuration," *IEEE Trans. Wireless Commun.*, vol. 13, no. 5, pp. 2614–2625, May 2014.

[15] M. López-Benítez, et al., "Time-dimension models of spectrum usage for the analysis, design, and simulation of cognitive radio networks," *IEEE Trans. Veh. Technol.*, vol. 62, no. 5, pp. 2091–2104, Jan. 2013.

[16] L. Stabellini, "Quantifying and modeling spectrum opportunities in a real wireless environment," in *Proc. IEEE Wireless Commun. Netw. Conf.*, 2010, pp. 1–6.

[17] ETSI, "Universal Mobile Telecommunications System (UMTS); selection procedures for the choice of radio transmission technologies of the UMTS", *TR UMTS 30.03, V3.2.0*, Apr. 1998.

[18] UMass Trace Repository, *ACM MMSys conference dataset archive*, (2013). [Online]. Available: http://traces.cs.umass.edu/index.php/Mmsys/Mmsys

[19] Qualcomm, "LTE in unlicensed spectrum: Harmonious coexistence with WiFi," White Paper, Jun., 2014.

[20] "Nokia LTE for unlicensed spectrum," White paper, Jun. 2014.

[21] IEEE 802.11, "Wireless LAN Media Access Control (MAC) and Physical Layer (PHY) specifications," *ANSI/IEEE Std., 802.11*, 1999.

[22] J. Jeon, et al., "LTE with listen-before-talk in unlicensed spectrum," in *Proc. IEEE Int. Conf. Commun. Workshop*, 2015, pp. 2320–2324.

[23] S. Y. Lien, et al., "Configurable 3GPP licensed assisted access to unlicensed spectrum," *IEEE Wireless Commun.*, vol. 23, no. 6, pp. 32–39, Dec. 2016.

[24] ETSI EN 301 893, "Broadband Radio Access Networks (BRAN); 5 GHz high performance RLAN; Harmonized EN Covering the Essential Requirements of Article 3.2 of the R&TTE Directive," *ETSI Std., V1.7.0*, Jan. 2012.

[25] S. R. Yang, et al., "Modeling UMTS power saving with bursty packet data traffic," *IEEE Trans. Mobile Comput.*, vol. 6, no. 12, pp. 1398–1409, Dec. 2007.

[26] Y. Chen and H.-S. Oh, "A survey of measurement-based spectrum occupancy modeling for cognitive radios," *IEEE Commun. Surv. Tut.*, vol. 18, no. 1, pp. 848–859, Jan.–Mar. 2016.

[27] S. Geirhofer, et al., "A measurement-based model for dynamic spectrum access in WLAN channels," *IEEE Mil. Commun. Conf.*, 2006, pp. 1–7.

[28] J. Janssen and R. Manca., *Applied Semi-Markov Processes*. Berlin, Germany: Springer, 2010.

[29] A. Nigam, et al., "Method and system for enabling discontinuous reception (DRX) over an unlicensed band in cellular networks," U.S. Patent Application No. 15/524,978, Nov. 2017.

[30] 3GPP TSG-RAN WG2 Meeting #57bis, Agenda item: 5.2.3 Nokia, "Evaluating DRX concepts for E-UTRAN; DRX parameters in LTE," *3GPP R2-071284, R2-071285*, St. Julian's, Malta, Mar. 2007.

[31] M. T. Kawser, et al., "Improvement in DRX power saving for non-real-time traffic in LTE," *ETRI J.*, vol. 38, no. 4, pp. 622–633, 2016.

[32] Y. Y. Mihov, et al., "Analysis and performance evaluation of the DRX mechanism for power saving in LTE," in *Proc. IEEE 26th Convention Electr. Electron. Eng. Israel*, 2010, pp. 520–524.

[33] C. S. Bontu, et al., "DRX mechanism for power saving in LTE," *IEEE Commun. Mag.*, vol. 47, no. 6, pp. 48–55, Jun. 2009.

[34] S. Y Lien, et al., "Random access or scheduling: Optimum LTE licensed-assisted access to unlicensed spectrum," *IEEE Commun. Lett.*, vol. 20, no. 3, pp. 590–593, Mar. 2016.

[35] R. Yin, et al., "A framework for co-channel interference and collision probability tradeoff in LTE licensed-assisted access networks," *IEEE Trans. Wireless Commun.*, vol. 15, no. 9, pp. 6078–6090, Sep. 2016.

[36] 3GPP TS 23.203, "Policy and charging control architecture" *Rel. 15, V.15.2.0*, Mar. 2018.

[37] J. M. Liang, et al., "An energy-efficient sleep scheduling with QoS consideration in 3GPP LTE-advanced networks for internet of things," *IEEE J. Emerging Sel. Topics Circuits Syst.*, vol. 3, no. 1, pp. 13–22, Mar. 2013.

[38] H. Bo, et al., "DRX-aware scheduling method for delay-sensitive traffic," *IEEE Commun. Lett.*, vol. 14, no. 12, pp. 1113–1115, Dec. 2010.

[39] P. M. Eittenberger, et al., "Monitoring mobile video delivery to android devices," in *Proc. 4th ACM Multimedia Syst. Conf.*, 2013, pp. 119–124.


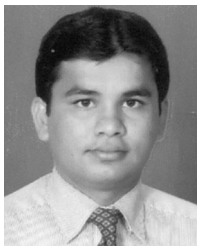

**Mukesh Kumar Maheshwari** received the bachelor's degree from the Mehran University of Engineering and Technology, Pakistan, and the master's degree from the University of Leicester, United Kingdom. He is currently working toward the PhD degree in the ECE Department of the College of Information and Communication Engineering, Sungkyunkwan University, South Korea. His research interests include 5G wireless communications and energy-efficient networks.

**Abhishek Roy** (S'03-M'09) received the MS degree from the University of Texas at Arlington, in 2002, and PhD degree from Sungkyunkwan University, Korea, in 2010. He is currently working as a principal engineer in the Network System Design Lab, Samsung Electronics, Korea. His research interests include resource and energy management in 5G wireless, IoT, social networking, and smart grids. He has served/is serving on the guest editorial and technical program committee of many international journals and conferences. He has co-authored one book (Taylor & Francis) and published more than 60 international journals. He is a member of the IEEE.

**Navrati Saxena** (S'03-M'09) received the PhD degree from the University of Trento, Italy. She is an associate professor and director of the Mobile Ubiquitous System Information Center (MUSIC), Sungkyunkwan University (SKKU), Korea. Prior to joing SKKU, she was an assistant professor with Amity University India and a visiting researcher with the University of Texas at Arlington. Her research interests involve 5G wireless, IoT, and smart grids. She has served/is serving on the guest editorial and technical program committee of international journals and conferences. She has co-authored one book (Taylor & Francis) and published more than 60 international journals. She is a member of the IEEE.